Egyptian Geophysical Society
EGS Journal, vol. 7, No. 1, 117-131 (2009)

USE OF GAMMA-RAY SPECTROMETRY IN OUTLINING FAVOURABLE SITES FOR POTENTIAL RADIOELEMENT CONCENTRATIONS, G. UMM ZARABIT AREA, CENTRAL EASTERN DESERT, EGYPT

M.A. GOUDA

Nuclear Materials Authority, P.O.Box 530 Maadi, Cairo, Egypt

استخدام معطيات المسح الاشعاعى الطيفى فى تحديد المواقع ذات القيمة لتركيزات العناصر الاشعاعية بمنطقة جبل أم زرابيت، وسط الصحراء الشرقية، مصر.

الخلاصة: تقع منطقة جبل أم زرابيت فى الجزء الأوسط من صحراء مصر الشرقية، تقريبا فى منتصف المسافة بين مدينتى سفاجا والقصير على ساحل البحر الأحمر وتشتمل المنطقة على صخور متنوعة : نارية ومتحولة ورسوبية تتراوح أعمارها من عصر ما قبل الكمبرى حتى الحديث ويعتمد تحليل بيانات المسح الاشعاعى الطيفى الحالى على تطبيق ثلاث تقنيات مختلفة للتفسير. التقنية الأولى ويتم بموجبها حساب دلائل توافق (مفاضلة) العناصر الاشعاعية الطيفية الثلاث (اليورانيوم، الثوريوم والبوتاسيوم) وذلك لتحديد أنسب المواقع المحتملة لاستكشاف العناصر المشعة وتعتمد التقنية الثانية وهى تقنية الصور المركبة على دمج تركيزات العناصر الاشعاعية الأساسية مع / أو نسبهم لانتاج خرائط ملونة مفسرة وتساعد تلك الخرائط فى تحديد نطاقات التمعدنات الاشعاعية العالية التى يمكن اعتبارها أهدافاً جيدة فى عمليات استكشاف الخامات المشعة وتوضح التقنية الثالثة مدى هجرة اليورانيوم القابل للتحرك من والى الصخور المختلفة بالمنطقة.

وقد أظهرت الدراسة أن محتوى الثوريوم أعلى من محتوى اليورانيوم فى غالبية الوحدات الصخرية تقريبا حيث بلغت أقصى قيم تم تسجيلها لمنطقة الدراسة حوالى ٥٤و٢٣ يو ار، ٤و٣ %، ٢٥و١٥ جزء فى المليون و ٧٨و١٨ جزء فى المليون وذلك لكل من العد الاشعاعى الكلى، نسبة البوتاسيوم، اليورانيوم المكافىء والثوريوم المكافىء بالترتيب وتوضح المستويات الاشعاعية المسجلة للوحدات الصخرية المختلفة المحتوى المعدنى الاشعاعى لها، وارتباط الشاذات الاشعاعية بصخور الكريتاوى العلوى و الأيوسين السفلى والجرانيت الحديث، كما أوضحت الدراسة أن معامل توافق اليورانيوم أظهر أن أعلى احتمالية لتواجد اليورانيوم ترتبط أساسا بصخور الجرانيت الحديث وما يلى الحمامات الفلسيتى، بينما ترتبط أعلى قيمة لمعامل توافق الثوريوم بصخور الميوسين الأوسط والكريتاوى العلوى. كما سجلت الدراسة أن أعلى معدلات لكمية اليورانيوم المهاجر من صخور المنطقة إلى خارجها ترتبط بصفة أساسية بصخور الجرانيت الحديث (– ٥٤و٨٣%) ومايلى الحمامات الفلسيتى (– ٧٤و٧٤%) ثم الدخان البركانى (– ٣٥و٦٥%) مما يشير إلى أهمية تلك الصخور كمصادر ذات قيمة لليورانيوم بمنطقة الدراسة.

ABSTRACT: *Gebel Umm Zarabit area is located in the central part of the Egyptian Eastern Desert, almost midway between Safaga and Quseir cities on the Red Sea coast. The area comprises a diversity of igneous, metamorphic and sedimentary rocks, ranging in age from Precambrian to Quaternary. The analysis of the present aeroradiospectrometric survey data relies essentially on three interpretation techniques. The first one is the computation of the three radioelements (U, Th and K) favourability indices for locating probable sites for radioelement exploration. The second one is the composite image technique which combines any three radioelement parameters and/or their ratios to generate interpretable composite colour image maps. These maps could help outline potential zones of anomalous radioelement content which may be considered as good targets for radioactive mineral exploration. Meanwhile, the third one is the uranium migration technique, which shows the amount of migrated uranium in and out of the different lithologic units.*

The study proved that eTh content is higher than eU content in nearly most rock types of the study area. The maximum readings recorded allover the mapped area reach about 23.54 Ur, 3.49%, 15.25 ppm and 18.78 ppm for TC., K, eU and eTh, respectively. The radiometric levels registered over the lithologically mapped units express their radioactive mineralization content and the mapped radiometric anomalies are spatially correlated with the Upper Cretaceous, Lower Eocene and the younger granitic rocks

Uranium favourability index shows relatively major probabilities of uranium potentiality associated with the younger granites and Post Hammamat felsites. Meanwhile, a high thorium favourability index was related to the Middle Miocene and Upper Cretaceous sediments. The maximum amount of uranium migration out-rate is connected with the younger granites (-83.54%), Post Hammamat felsites (-74.74%) and Dokhan volcanics (-65.35%). This may draw attention to their importance as U-source bodies in the study area.

INTRODUCTION

Gebel (G) Umm Zarabit area is located in the central part of the Eastern Desert of Egypt, almost midway between Safaga and Quseir cities on the Red Sea coast. It is enclosed between latitudes 26° 19\ 30\\ and 26° 30\ 00\\ N, and longitudes 33° 48\ 30\\ and 34° 02\ 00\\ E (Fig. 1) . So, it has nearly a square shape covering about 440 km^2, mostly composed of crystalline basement rocks. The area is characterized by both gentle and rough topography. It is traversed by many wadis having a general NE trend, roughly at right angle to the Red Sea axis, with NW trend also common (Fig. 2). The general outline of the drainage system shows a dendritic pattern. The area is dissected by some of famous wadis including W. Umm Zarabit, Wadi Abu-Aqarib, W. Abu-Safi, W. Umm Esh, W. Abu-Shiqeili, W. Gasos and W. Saqia. These wadis either drain to the Nile River at the west or to the Red Sea to the east.

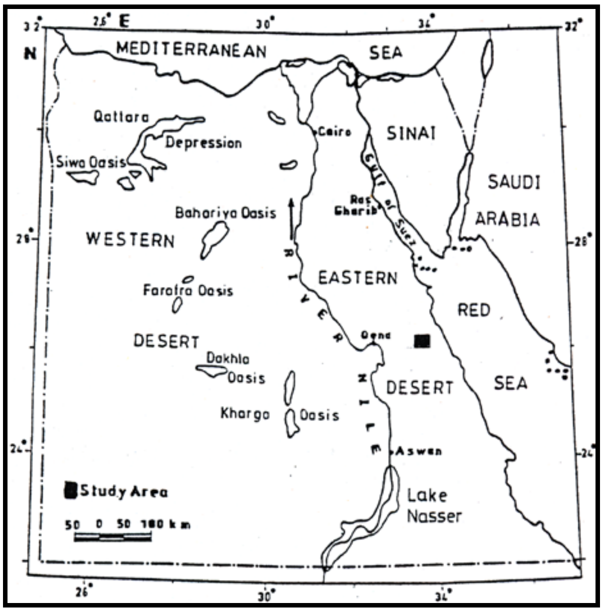

Fig. (1): Map of Egypt showing the location of G. Umm Zarabit area, Central Eastern Desert, Egypt.

The area under consideration has been involved in the aerial multi channel gamma-ray spectrometric and magnetic survey conducted by Aero-Service Division, Western Geophysical Company of America, in 1984, over a large territory of the Eastern Desert of Egypt. The aerial radiospectrometric measurements were made by a continuously-recording airborne high sensitivity 256-channel gamma-ray spectrometer having 50 litres NaI "TL" detector.

The outlining of the favourable sites for potential economic radioactive mineral deposits together with studying the nature of the concentration of the causing radioisotopes and the relationship that might exist between the distribution of these probable radioactive provinces and their relation to the geological features have formed the basis and main objective for the present work. This objective is accomplished by examining the spectral gamma-ray data in conjunction with the topography, geology and structure of the study area.

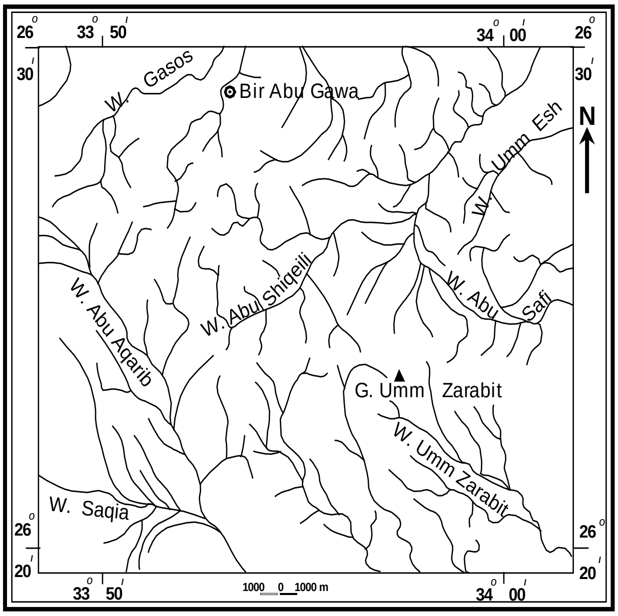

Fig. (2): Drainge pattern of G. Umm Zarabit area, Central Eastern Desert, Egypt.

GEOLOGICAL OUTLINE

The study area comprises a wide diversity of igneous, metamorphic and sedimentary rocks, ranging in age from the Precambrian to Quaternary. The different exposed rocks are chronologically grouped into the following sequence, from the oldest to youngest, according to the classifications and works of El-Ramly, 1972, El-Shazly, 1977, El-Shazly et al., 1980, Akaad and Noweir, 1980, El-Gaby et al., 1988 & 1990, and Conoco Coral, 1989. The distribution of the different rock types in the study area is given on the compiled geological map (Fig. 3) prepared mainly from the geological map of the Qena quadrangle, 1978 published by the Egyptian Geological Survey and Mining Authority (EGSMA) and the photogeological interpretation map, sheet 14, published by Conoco, 1986.

Dokhan Volcanics: They are mainly of intermediate to acidic composition and are represented by non-metamorphosed andesites, porphyrites, pyroclastics and the well-known purple-coloured Imperial porphyry. These volcanics are well-developed, widely distributed and are mainly cropping out in the central and southern parts of the study area, respectively to the east and south of G. Um-Zarabit.

Hammamat sediments: These sediments are occurring as relatively large masses occupied the southeastern corner, the northeastern part to the north of G. Um-Zarabit and in the weastern part to the east of W. Abu-Aqarib. They are essentially unmetamorphosed conglomerate, greywacke, arenite and siltstone.

Post Hammamat felsites: Post Hammamat felsites include the effusive felsite porphyry bodies, sheets, plugs and breccias, which are common associates of the Hammamat group. They are of limited distribution in the mapped area and mainly cropping out as small scattered masses in the north central part, besides two small exposures in the southeastern and western parts.

Younger granites: They are represented by intrusive granites possessing sharp contacts with the surrounding rocks; their majorities are believed to be formed by the end of Late Precambrian times. They are coarse-grained rocks greatly variable in composition and composed mainly of quartz, potash feldspars, in addition to some plagioclase feldspars and subordinate biotite and hornblende. These granites form the main mass of G. Umm Zarabit in the eastern part of the area, in addition to small outcrop around W. Gasos in the northwestern part.

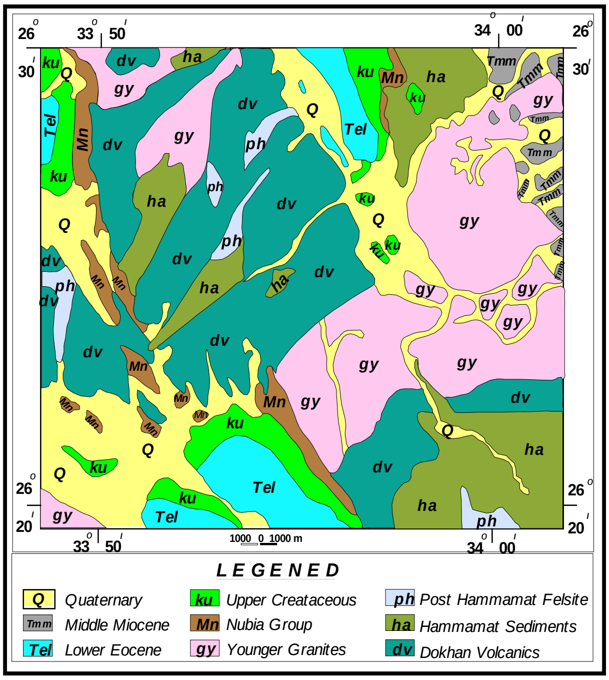

Fig. (3): Compiled geological map of G. Umm Zarabit area, Central Eastern Desert, Egypt.

Mesozoic Nubian group: This group of sediments includes Campanian Taref sandstone and Quseir variegated shale. In the present area, these sediments are represented by limited occurrences in the form of elongated belts along the western side of the area running generally in a NW direction.

Upper Cretaceous: They are represented by small separate scattered outcrops along the northern, southern and northwestern parts of the mapped area and composed mainly of alternating thin beds of phosphate, shale, marlstone and oyster limestone.

Lower Eocene: These sediments are composed mainly of yellow to white thick limestone section containing chert concretions designated as Thebes Formation. The upper part of the underlying Esna shale is recorded at the base. In the studied area, they are of limited distribution and mainly exposed as small masses in the southern and northern parts, in contact with the Upper Cretaceous sediments.

Middle Miocene: Includes fluviatile and continental clastics as well as gypsum, anhydrite, celestite and salt deposits. Rocks of this group are of limited distribution and represented by small exposures occupied the northeastern corner of the area.

Quaternary: They are represented by the quaternary wadi sediments which constitute the surficial cover in the main wadis and their tributaries. These sediments are composed of loose sands, detritus, gravels, pebbles, cobbles and rare boulders.

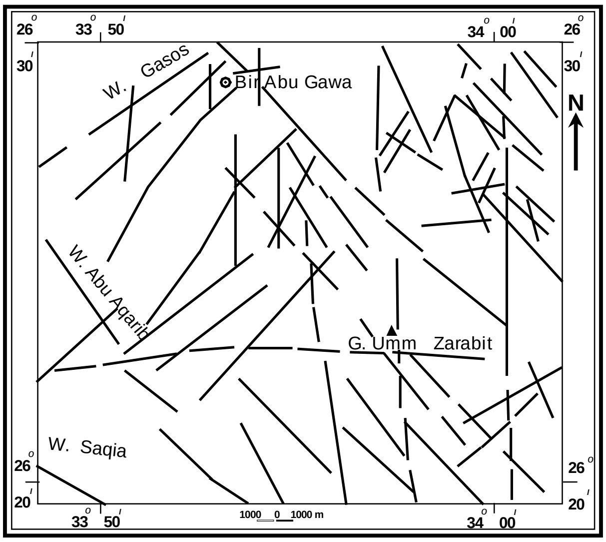

Fig. (4): Surface structural lineaments as deduced from the geological map, G. Umm Zarabit area, Central Eastern Desert, Egypt.

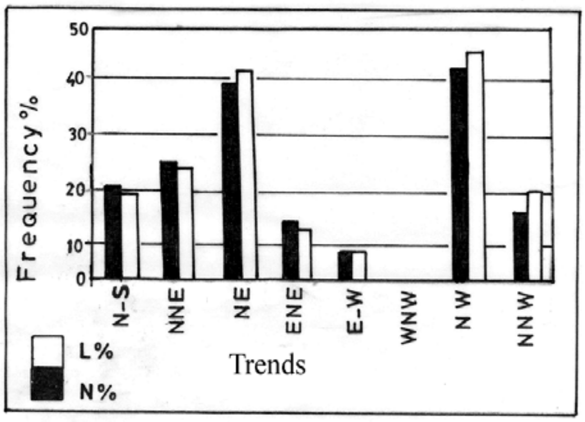

Fig. (5): Vertical bar chart showing length and numbers of relative frequency distributions of the surface structural lineaments as traced from the geological map, G. Umm Zarabit area, Central Eastern Desert, Egypt.

Surface structural lineaments, as traced from the geological map (Fig. 3) of the study area are illustrated in Fig. (4) and have been statistically analyzed with respect to their number and length proportions. The interpreted surface structural trends were grouped into the eight main categories according to its direction from east to west. The result of this study is given in the vertical bar chart (Fig. 5) which shows the length and number of the relative frequency distributions of these structural lineaments. It is evident from this figure that major linear trends were found to take mainly the NW and NE directions. Some other trends that take the N-S, NNW, NNE and ENE directions could be also detected but with less significance.

Data analysis and interpretation

The gamma-ray spectrometric data were qualitatively and quantitatively interpreted in order to distinguish between various lithologic units as regards their radioelement concentrations. Since 1980's, the enhancement of gamma-ray spectrometric data has benefited from digital image processing techniques. Nevertheless, the traditional presentation methods, such as profiles and contour maps, have their advantages, and are still in common use (IAEA, 2003). The interpretation of the gamma-ray spectrometric maps of the study area depends mainly upon the excellent correlation between the general patterns of the recorded radioactivity measurements and surface distribution of the various types of rock units and exposures. This correlation has been interpreted according to the radiometric units inferred from the different radiometric levels and this has been achieved from the experience gained in neighbouring areas. So, the investigation of the different aeroradio-spectrometric maps together with the compiled geological map was regarded as the starting point for qualitative and, later, quantitative interpretations to establish the general levels of radioactivity for the different rock types recorded in the study area. The distribution of these levels at the surface is controlled by bedrock composition and modified by a variety of geologic processes, the most dominant being weathering, erosion and transportation (Pitkin and Duval, 1980). Naturally, these radiometric levels are not by any means always sharp, but merge into one another to various degrees. Over some rock units, the coincidence of the radiometric boundaries with the lithologic ones was excellent, while over some others was relatively poor.

The close examination of the four spectral radiometric variable maps (T.C., K, eU and eTh; Figs. 6 to 9) reveals a wide variation and broad range of aeroradioactivity which reflect the fact that the area under study is surfaced almost totally by exposed basement rocks of different composition. It is evident from the correlation between the different rock units and the recorded levels of gamma-radiation that-on regional scale-the pattern of aeroradioactivity is closely connected with the surface geology of the area under investigation. Generally, the younger granitic rocks together with the Upper Cretaceous and Lower Eocene sediments manifest the highest radioelement concentrations within all the rock units in the mapped area. Meanwhile, the lowest concentrations are restricted to the Hammamat sediments and Dokhan volcanics. The intermediate radioactivity level is mainly associated with the Quaternary and Post Hammamat felsites.

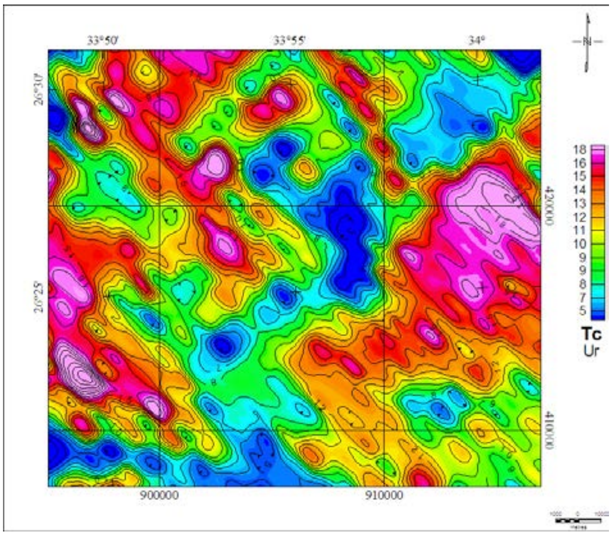

Fig. (6): Total count filled coloured contour map (in Ur), G. Umm Zarabit area, Central Eastern Desert, Egypt.

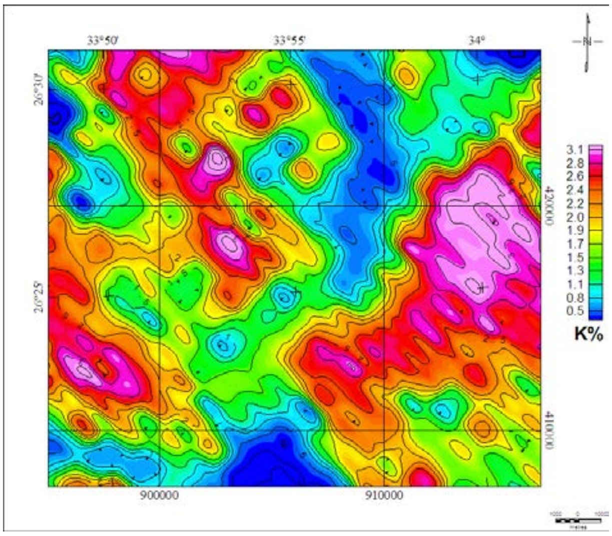

Fig. (7): Potassium filled coloured contour map (in %), G. Umm Zarabit area, Central Eastern Desert, Egypt.

It has been recognized that the different radiospectrometric maps (T.C., K. eU and eTh) display nearly the same colour zonations and show great similarities concerning the general features, gradients of contour lines as well as the distribution and trends of the anomalies. The most prominent radiospectrometric feature that could be drawn out from these maps (Figs.

6 to 9) is the steep gradients which run nearly in the NW, NNW and NE directions. These gradients reflect the probable presence of faulting systems that run in these directions. Such interpreted radiometric structural lineaments could be correlated with the fault systems shown on the compiled geological map (Fig. 4). The distribution of the radioelements in the study area may be associated with dykes and/or veins running parallel to the prevailing fractures and faults especially those directed in the NW and NE directions or at their intersection zones.

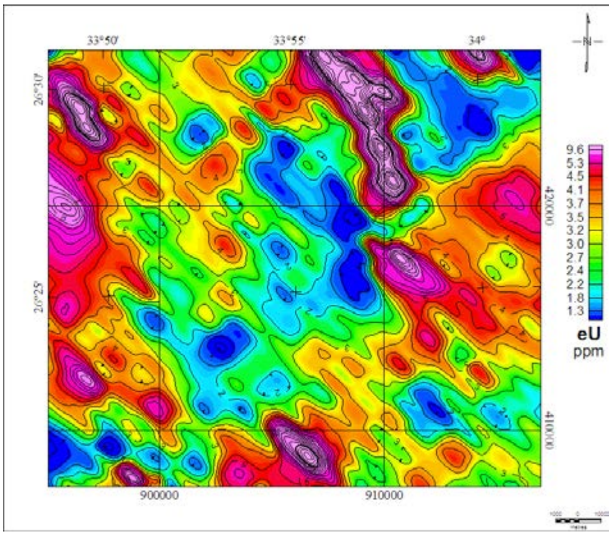

Fig. (8): Equivalent uranium filled coloured contour map (in ppm), G. Umm Zarabit area, Central Eastern Desert, Egypt.

From Table (1) it can be seen that, the total count map (Fig. 6) displays a range of radioactivity varying from about 1.79 Ur over the Quaternary sediments located to the north of W. Umm Esh in the northeastern corner of the study area, to about 23.54 Ur over the Mesozoic Nubian group in the southwestern corner to the north of W. Saqia, with an average value of about 11.01 Ur (1Ur = unit of radioelement concentration = 1 ppmeU = 0.6 ųR/h). The eU map (Fig. 8) reaches about 15.25 ppm as a maximum value over the Upper Cretaceous sediments north of W. Abu Aqarib in the northwestern part of the area and diminishes to 0.22 ppm over the Quaternary alluvium north of G. Umm Zarabit in the central part of the area. The average abundance of eU in the study area-as a whole-attains about 3.52 ppm. The eTh (Fig. 9) reaches its maximum value of about 18.78 ppm and seems to be associated with the Middle Miocene sediments located at the southwestern part of the study area to the north of W. Saqia. Meanwhile, the minimum eTh concentration reaching about 1.03 ppm is associated with the Quaternary alluvium in the northeastern corner to the north of W. Umm Esh. The average abundance of eTh is about 6.41 ppm for the whole of the study area. Potassium content as indicated in Fig. (7) ranges from 0.26 which is associated with the Middle Miocene sediments in the northeastern corner to the north of W. Umm Esh, to about 3.49% recorded over the Dokhan volcanics north of W. Abu Shiqeili in the north central part of the mapped area. The average abundance of K is about 1.81%.

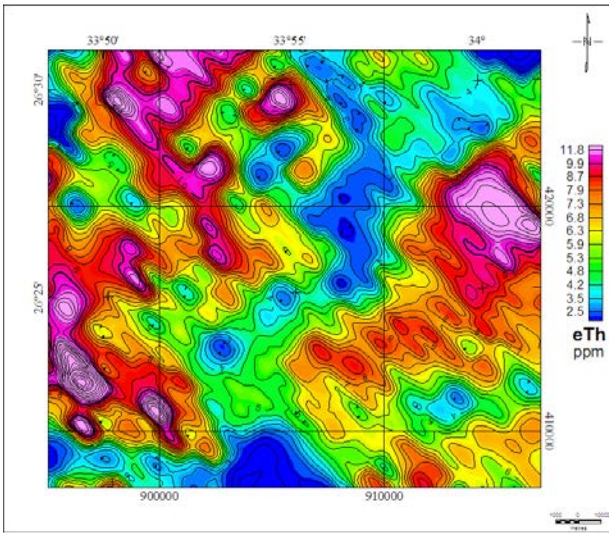

Fig. (9): Equivalent thorium filled coloured contour map (in ppm), G. Umm Zarabit area, Central Eastern Desert, Egypt.

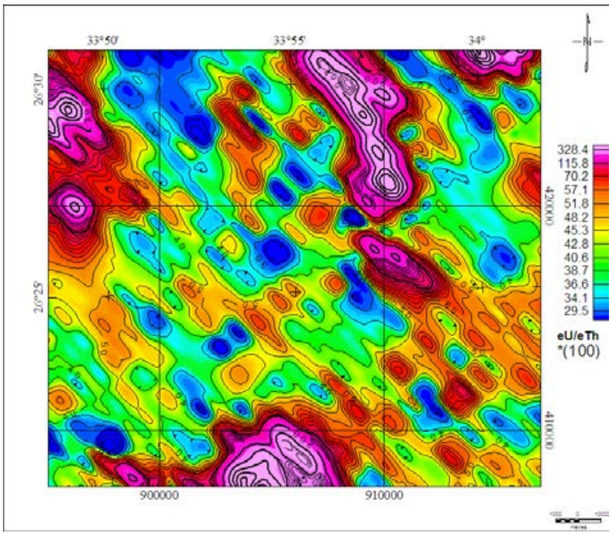

Fig. (10): eU/eTh filled coloured ratio contour map (in ppm/ppm), G. Umm Zarabit area, Central Eastern Desert, Egypt.

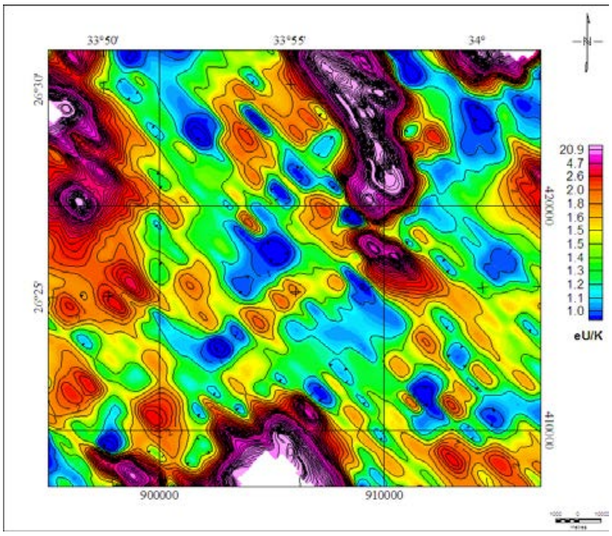

Fig. (11): eU/K filled coloured ratio contour map (in ppm/%), G. Umm Zarabit area, Central Eastern Desert, Egypt.

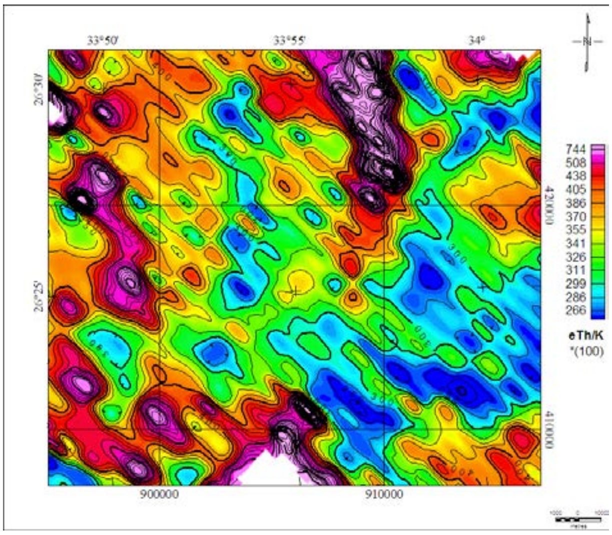

Fig. (12): eTh/K filled coloured ratio contour map (in ppm/%), G. Umm Zarabit area, Central Eastern Desert, Egypt.

It must be borne in mind that the observed measurements of the three radioelements are taken from air using airborne gamma-ray spectrometer at a nominal sensor altitude of 120 meters terrain clearance. So, the detected concentrations have been greatly attenuated because of the long distance between the ground and the detector used. Accordingly, the recorded aerial radioelement measurements show much less values than that of the actual surface concentrations.

It is obvious from Table (1) that, except the Upper Cretaceous and Lower Eocene sediments, the lithologic units of the study area exhibit eTh contents more than the eU ones. As a result, the eU/eTh ratio (Fig. 10) records its lowest values over younger granites, Dokhan volcanics, Post Hammamat felsites and Hammamat sediments (0.45, 0.46, 0.48 and 0.53), respectively. This ratio increases against the other rock units to reach its maximum values (1.01, 1.31 and 1.63) over the Middle Miocene, Upper Cretaceous and Lower Eocene sediments respectively, where thorium contents are decreased and the uranium contents may be slightly increased as a result of uranium precipitation or migration into these units. In addition, all the lithologic units of the study area have eTh/K values (Fig. 12) more than 3, which means that they are thorium rich according to Ong and Mior Shallehhuddin, 1988, who reported that if eTh/K≥2 the rock is thorium rich.

STATISTICAL TREATMENT

The gamma-ray spectrometric data of the four radiometric variables (T.C., K. eU and eTh) measured over the study area besideS three of their ratios (eU/eTh, eU/K and eTh/K) have been subjected to statistical analysis in order to draw valid conclusions and extract reasonable predictions regarding the nature and significance of the distribution of the radioelements in the area. It is worthy to mention that statistical analysis of the aerial spectrometric data has been performed in terms of the individual rock types to avoid errors in geological mapping. Statistical computations were applied on the original data without employing any type of transformation. In this regard, minimum (min.), maximum (max.), arithmetic mean (X) and standard deviation (S) were computed for the different radiospectrometric parameters in the different rock units. The results are illustrated in Table (1). In addition, the normality and the degree of homogeneity of the distributions has been tested by calculation of the coefficient of variability (C.V. = S/X*100) for each radiometric parameter of the different rock types. If C.V.% value of a certain

Unit is less than 100%, the unit exhibits normal distribution (Sarma and Koch, 1980).

Locating Favourable Areas For Radioelement Exploration

In the past, most interpretation efforts were directed towards explaining, classifying and setting priorities on gamma-ray spectrometric anomalies to aid exploration. However, locating favourable areas in the first place is another problem. Reconnaissance surveys can outline large regions with above average radioelement content (geochemical provinces), which may be considered favourable areas, or in the vicinity of favourable areas (Darnley et al., 1977).

Saunders and Potts (1978) attempted to determine a general "uranium favourability index" by plotting histograms of various possible indices such as the eU/eTh ratio for about 30 different areas where existing mines and occurrences were known to be favourable. They concluded that the median values of aerial gamma ray spectrometer parameters for geologic map units could be used as a guide to identify uraniferous

Table (1): Results of the statistical treatment of airborne gamma-ray pectrometric data, G. Umm Zarabit area, Central Eastern Desert, Egypt

Rad. Par.	Quaternary (295)					Middle Miocene (29)				
	Min.	Max.	X	S	C.V.	Min	Max.	X	S	C.V.
T.C. (Ur)	1.79	23.52	10.88	3.90	35.85	3.02	19.71	10.86	3.60	33.15
K(%)	0.28	3.31	1.70	0.76	44.67	0.26	3.17	1.62	0.82	50.62
eU(ppm)	0.22	14.97	4.28	2.08	48.60	0.83	11.09	4.08	2.19	53.68
eTh(ppm	1.03	18.70	5.01	2.84	56.69	1.71	13.15	5.82	2.73	46.91
eU/eTh	0.09	5.99	0.70	0.66	94.29	0.23	6.03	1.01	0.94	93.07
eU /K	0.37	51.99	3.25	2.98	91.69	0.65	33.82	4.81	4.13	85.86
eTh /K	2.09	12.16	4.08	1.22	29.90	2.38	6.41	3.90	0.94	24.10
Rad. Par.	Lower Eocene (61)					Upper Cretaceous (76)				
	Min.	Max.	X	S	C.V.	Min	Max.	X	S	C.V.
T.C. (Ur)	4.15	15.49	8.25	2.53	30.67	3.81	17.61	9.87	2.97	30.19
K (%)	0.26	2.20	0.82	0.44	53.66	0.26	2.49	1.13	0.54	47.78
eU (ppm)	1.45	13.33	4.38	3.13	71.46	0.91	15.25	5.19	3.59	69.17
eTh (ppm)	1.41	7.52	3.97	1.26	31.74	1.61	11.70	4.57	1.57	38.29
eU / eTh	0.28	4.88	1.63	1.21	74.23	0.18	5.32	1.31	1.20	91.60
eU / K	1.08	36.43	9.48	8.26	87.13	0.82	42.69	7.69	5.96	77.50
eTh / K	2.86	9.48	4.95	1.49	30.10	2.75	10.20	4.87	1.70	34.90
Rad. Par.	Mesozoic Nubian group(53)					Younger granites (317)				
	Min.	Max.	X	S	C.V.	Min	Max.	X	S	C.V.
T.C. (Ur)	5.43	23.54	11.52	3.63	31.51	2.50	20.31	12.74	3.71	29.12
K (%)	0.36	3.18	1.58	0.56	35.44	0.43	3.39	2.30	0.70	30.00
eU (ppm)	1.66	14.87	4.70	2.76	58.72	0.49	14.35	3.28	1.37	41.76
eTh (ppm)	2.95	18.78	6.83	2.52	36.89	1.64	13.97	7.43	2.45	32.97
eU / eTh	0.31	4.58	0.75	0.57	76.0	0.17	4.30	0.45	0.26	56.52
eU / K	1.14	37.86	3.74	3.22	86.10	0.47	33.14	1.53	1.42	92.81
eTh / K	2.90	9.61	4.61	1.42	30.80	2.21	11.18	3.26	0.64	19.63
Rad. Par.	Post Hammamat felsites (33)					Hammamat sediments (176)				
	Min.	Max.	X	S	C.V.	Min	Max.	X	S	C.V.
T.C. (Ur)	5.45	19.20	13.56	3.22	23.74	5.12	17.41	10.47	2.46	23.49
K (%)	0.95	3.32	2.22	0.52	23.42	0.33	3.29	1.78	0.54	30.33
eU (ppm)	1.59	5.61	3.84	1.08	28.12	0.80	12.62	3.03	1.60	52.80
eTh (ppm)	3.04	12.50	8.29	2.28	27.50	2.85	11.29	6.19	1.81	29.24
eU / eTh	0.24	0.83	0.48	0.11	22.91	0.15	3.60	0.53	0.44	83.01
eU / K	0.76	2.77	1.77	0.45	25.42	0.44	37.78	2.31	2.19	94.81
eTh / K	2.69	5.39	3.74	0.56	14.97	1.98	10.90	3.66	1.10	30.05
Rad.Par.	Dokhan Volcanics (392)									
	Min.	Max.	X	S	C.V.					
T.C. (Ur)	2.80	19.31	10.88	3.28	30.14					
K (%)	0.48	3.49	1.70	0.59	34.71					
eU (ppm)	0.31	10.30	2.98	1.01	33.89					
)eTh (ppm	2.00	14.05	5.57	2.21	39.68					
eU / eTh	0.14	1.48	0.46	0.12	26.66					
eU / K	0.48	6.14	1.56	0.51	32.69					
eTh / K	2.10	7.56	3.47	0.66	19.02					

Rad. Par. = radio-spectrometric parameter
( ) number of measurements
Min. = minimum
Max. = maximum
X = arithmetic mean
S = standard deviation
C.V. = coefficient of variability

provinces, reasoning that where the crustal abundance of uranium is high it is available to be chemically concentrated in economic deposits. They further reasoned that geochemical processes must have concentrated a part of the uranium in deposits. Removal of uranium from average rocks, separating it from thorium and potassium, results in low eU/eTh and eU/K median values.

Based on the observation that high mean uranium content indicates that there is sufficient uranium for possible geochemical concentrating processes to work, and that low mean eU/eTh and eU/K values indicate that these processes took place, they derived the index U_2 for uranium.

$$U_2 = MeU / [(MeU/MeTh) * (MeU/MK)]$$

$$= MeTh * MK / MeU \qquad (1)$$

where M denotes the mean value. It is to be noted that a high value of U_2 indicates a high potential of uranium.

Then, the other two indices for thorium and potassium potentialities can also be derived (Ammar, et. al., 1999) to relate the three radioelements in a different way than the U_2 parameter as follows:

$$Th_2 = (MeU * MK) / (MeTh) \qquad (2)$$

and

$$K_2 = (MeU * MeTh) / (MK) \qquad (3)$$

This technique is designed primarily to identify all zones of primary enrichment within the country rocks, and secondly to indicate, if possible, the limits of areas where secondary processes have operated. It is important not to dismiss anomalous areas as simply being low-grade igneous rocks of no economic importance. Such areas may have considerable potential as source areas, and geological knowledge must be brought into consideration to determine where the eroded materials from these source areas have been deposited (Saunders and Potts, 1978). It is the first objective of this interpretation technique to delineate as rapidly as possible the major locations of radioelements enrichment in the area under study.

Calculations of these three indices have been carried out to locate rocks having the highest radioelements potentialities. A high index indicates high potential for radioactive elements. Accordingly, these areas will be considered as promising exploration targets either for radioactive mineral deposits and/or associated non-radioactive deposits.

Although the principle of favourability index was based on data obtained from areas known to have workable uranium deposits in Canada, there is some logic for using it to throw light on areas without such economic uranium contents. The histograms in (Fig. 13 a, b and c) show the vertical bar charts of radioelements favourability indices for the whole rock units forming Umm-Zarabit area.

***(1) Uranium favourable lithologic units*:**

The rock units forming G. Umm Zarabit area could be-roughly-classified into three main groups as far as their uranium favourability indices are relatively concerned, and as far as the study area is concerned (Fig. 13 a & Table 5). The first group outlines the units that possess relatively major probability of uranium potentiality with uranium favourability index value equal to or more than 4.79. It includes younger granites and post-Hammamat felsites. These units require further verification and research. The second group indicating the units of relatively moderate potential for uranium with U-index value ranging from 2.89 to 3.64 and includes essentially the units of Quaternary alluvium, Dokhan volcanics and Hammamat sediments. The third and last group displays the relatively minor probability of uranium with U-index values equal to or lower than 2.31, which includes the Lower Eocene, Upper Cretaceous, Mesozoic Nubian group and Middle Miocene units. Uranium favourability zones with related spectrometric values and associated rock types have been given in Table (2).

***(2) Thorium favourable lithologic units*:**

According to the calculated thorium favourability index-values, the rock units of G. Umm Zarabit area could be classified into three main groups of relatively major, moderate and minor potentials (Fig. 13 b & Table 5). The major potential group, with a Th-index value equals to or more than 1.14 and includes the Middle Miocene and Upper Cretaceous. The moderate potential with a Th-index value ranging from 1.02 to 1.09 and correlated with younger granites, post Hammamat felsites and Mesozoic Nubian group. The minor or least potential thorium favourability index (≤ 0.99) is associated with the Hammamat sediments, Dokhan volcanics, Lower Eocene and Quaternary. Thorium favourability zones with related spectrometric values and associated rock types are shown in Table (3).

Efimov (1978) who quantified this parameter showed that it can acquire values up to 1.2 or 1.3 in common non-altered rocks, while in altered rocks it may be 2 or even 5, exceptionally 10. Moreover, its statistical stability is better than that of the eTh/eU ratio. Concerning the study area, the calculated values of this parameter for the different rock types were found to oscillate between 0.78 and 1.2, which may indicate that the mapped area has not been much influenced by alteration processes.

***(3) Potassium favourable lithologic units*:**

Three main groups of relatively minor, medium and major potentials, could be distinguished in the study are based on their calculated potassium favourability index (Fig. 13 c & Table 5). The major potential, with a K-index value equal to or grater than 20.32 is correlated with the Mesozoic Nubian group, Lower Eocene and Upper Cretaceous.

Table (2): Uranium favourability zones with related spectrometric values and associated rock types, G. Umm Zarabit area, Central Eastern Desert, Egypt.

Favour. zones	Rock type	U_2- index			K (%)			eU (ppm)			eTh (ppm)		
		mean	min.	max.	mean	min.	max.	mean	min.	max.	mean	min	max.
Minor Potintial	Tel, Ku Mn & Tmm	1.60	0.74	2.31	1.29	0.26	3.18	4.59	0.83	15.25	5.30	1.41	18.78
Moderate Potintial	Q, dv & ha	3.24	2.89	3.64	1.73	0.28	3.49	3.43	0.22	14.97	5.59	1.03	18.70
Major Potintial	gy & ph	5.00	4.80	5.21	2.26	0.43	3.39	3.56	0.49	14.35	7.86	1.64	13.97

Table (3): Thorium favourability zones with related spectrometric values and associated rock types, G. Umm Zarabit area, Central Eastern Desert, Egypt.

Favour. zones	Rock type	Th_2- index			K (%)			eU (ppm)			eTh (ppm)		
		mean	min.	max.	mean	min.	max.	mean	min.	max.	mean	min.	max.
Minor Potintial	ha, dv Q & Tel	0.91	0.87	0.99	1.50	0.26	3.49	3.67	0.22	14.97	5.19	1.03	18.70
Moderate Potintial	gy, ph &Mn	1.05	1.02	1.09	2.03	0.36	3.39	3.97	0.49	14.87	7.52	1.64	18.78
Major Potintial	Tmm & Ku	1.17	1.14	1.20	1.38	0.26	3.17	4.64	0.83	0.91	5.20	1.61	13.15

Table (4): Potassium favourability zones with related spectrometric values and associated rock types, G. Umm Zarabit area, Central Eastern Desert, Egypt.

Favourable Zones	Rock type	K_2- index			K (%)			eU (ppm)			eTh (ppm)		
		mean	min.	max.	mean	min.	max.	mean	min.	max.	mean	min.	max.
Minor Potintial	dv, ha & gy	10.20	9.47	10.60	1.93	0.33	3.49	3.11	0.31	14.35	6.41	1.64	14.05
Moderate Potintial	Ph, Q &Tmm	14.49	14.34	14.66	1.85	0.26	3.32	4.07	0.22	14.97	6.37	1.03	18.70
Major Potintial	Mn, Ku & Tel	21.30	20.32	22.37	1.18	0.26	3.18	4.76	0.91	15.25	5.12	1.41	18.78

Table (5): Three radioelement favourability indices in different rock units, G. Umm- Zarabit area, Central Eastern Desert, Egypt.

Rock units	favourability indices		
	U_2	Th_2	K_2
Q	2.89	0.99	14.47
Tmm	2.31	1.14	14.66
Tel	0.74	0.90	21.21
Ku	1.06	1.20	22.37
Mn	2.30	1.09	20.32
gy	5.21	1.02	10.60
ph	4.80	1.03	14.34
ha	3.64	0.87	10.54
dv	3.18	0.88	9.47

U_2 = uranium favourability index

Th_2 = thorium favourability index

K_2 = potassium favourability index

Q = Quaternary,

Tmm = Middle Miocene,

Tel = Lower Eocene,

Ku = Upper Cretaceous,

Mn = Nubian group,

gy = younger granites,

ph = post Hammamat felsites

ha = Hammamat sediments,

dv = Dokhan volcanics

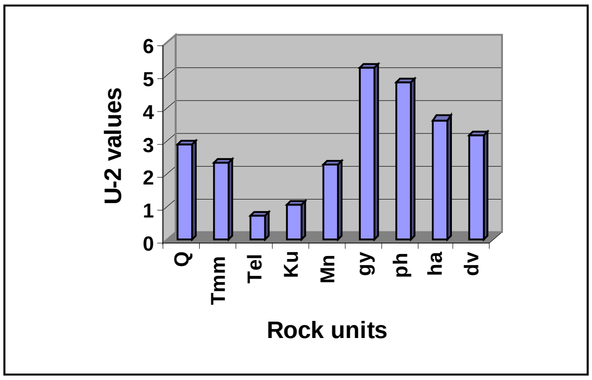

(A)

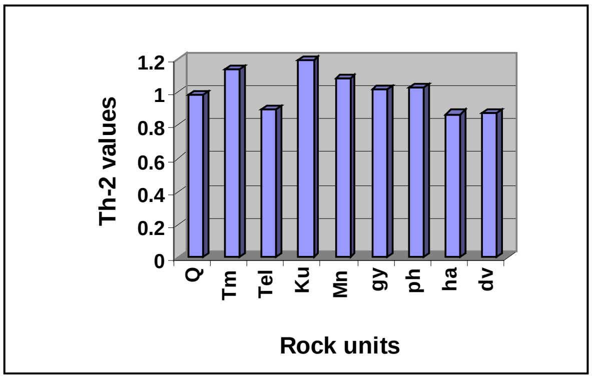

(B)

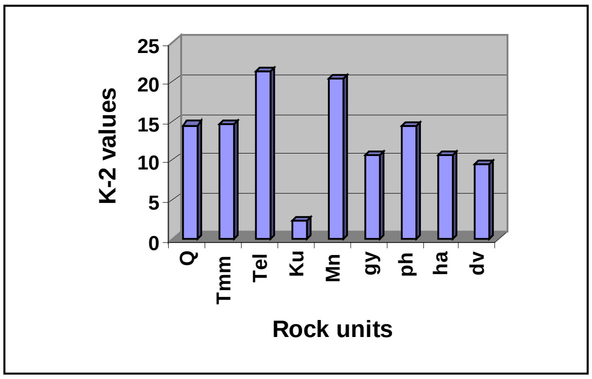

(C)

Fig (13): vertical bar chart showing the three radioelement indices: (a): U_2, (B): Th_2 and (C): K_2 , for the different rock units forming G.Umm- Zarabit area, Central Eastern Desert, Egypt.

The moderate potential, with a K-index value (from 14.34 to 14.66) could be associated with the Post Hammamat felsites, Quaternary alluvium and Middle Miocene sediments. The last group that displays the relatively minor potentiality of potassium, with a K-index value equal to or less than 14.66, includes Dokhan volcanics, Hammamat sediments and younger granites.

Uranium Migration In Different Geological Units

Due to their similar ionic radii, uranium and thorium are often associated in geologic units and formed under the same condition in the magma chamber. The uranium is easy to mobilize and migrate under the action of oxygen from groundwater and atmosphere during its evolution, whereas thorium is relatively stable in the oxidation zones, and stays in place. This means that the present Th-high area could be considered as the original U-high area.

The U/Th ratio is a very important geochemical index for U migration. It is approximated by a constant in the same rock type or geologic unit in a relatively closed environment. The Uranium migration (out or in) has the same probability within geological units in relatively closed geologic environment. On the other hand, the variations in the U/Th ratios reflect the extent of U migration in or out of this environment. Analysis of uranium migration is shown from the following steps in form of calculation of:

1-Paleo-uranium background (original uranium content Uo), which means multiplying the average Th content detected in each geologic unit by average regional U/ Th ratio (Benzing Uranium Institute, 1977 and NMA report, 1999).

Uo = eTh . U/ Th . . . . . . (1)

where eTh is the average thorium content in a certain geologic unit (ppm); U/ Th means the average regional U/ Th ratio in different geologic units.

2- Amount of mobilized Uranium (i.e. amount of uranium migration Um).

Um = Up - Uo . . . . . .…. (2)

where Up means average uranium content in certain geologic unit.

If Um > 0, uranium migrated in to the geologic body during late evolution .

If Um < 0, uranium was lost in the geologic body during late evolution .

3- Calculate the mobilized uranium migration rate (P).

P = Um / Up*100% . .. .(3)

The geologic units with negative amount of uranium migration can be considered as uranium source bodies, which provide uranium mineralization in the present area. Accordingly, from table (6) it can be shown that the maximum amount of uranium migration-out rate is connected with the younger granitic rocks (-83.54%), which indicates that they could be represented as a major U-source body in the study area. Moreover, Post Hammamat felsites together with the Hammamat sediments and Dokhan volcanics display uranium migration-out rates of about -74.74%, -65.35% and -51.34% respectively, which may draw attention also to their importance as U-source bodies in the present area, but in less significant amount than the granitic rocks. The minimum value of uranium migration-out rate (-15.44%) is recorded with the Middle Miocene sediments.

On the other hand, from table (6) the Upper Cretaceous, Lower Eocene sediments and Quaternary alluvium are found to have original uranium content values of about 3.70, 3.22 and 4.06 respectively. Consequently, their uranium migration rates are 28.71%, 26.48% and 5.14% respectively. According to this result, these three units could be considered as uranium migration-in units.

Table (6): Statistics for uranium migration in different rock units, G.Umm Zarabit area, Central Eastern Desert, Egypt.

Rock units	(Up)	(Uo)	(Um)	(P)
Q	4.28	4.06	0.22	5.14
Tmm	4.08	4.71	-0.63	-15.44
Tel	4.38	3.22	1.16	26.48
Ku	5.19	3.70	1.49	28.71
Mn	4.70	5.53	-0.83	-17.66
Gy	3.28	6.02	-2.74	-83.54
Ph	3.84	6.71	-2.87	-74.74
Ha	3.03	5.01	-1.98	-65.35
Dv	2.98	4.51	-1.53	-51.34

(Up) = Present uranium (Uo) = Original uranium

(Um) = Migrated uranium (P) =Uranium migration rate

COMPOSITE IMAGING

False colour composite images produced from the aerial gamma-ray spectrometric data sets can be used merely to demonstrate their importance as an aid for geological and geochemical mapping, on a regional scale, as well as for mineral exploration purposes

(Broom, 1990 & Elsirafy, et al., 1995). These images are generated by assigning a different primary colour to each data set, and then superimposing the results. Using primary colours, the numbers of data sets that can be combined is limited to three. Four different composite colour image maps were prepared for the following variable combinations:

1- eU, eTh and K (absolute three radioelement composite image map, Fig. 14).
2- eU, eU/eTh and eU/K (equivalent uranium composite image map, Fig. 15).
3- eTh, eTh/eU and eTh/K (equivalent thorium composite image map, Fig. 16).
4- K, K/eU and K/eTh (potassium composite image map, Fig. 17).

The absolute radioelement composite colour image provides a view of the overall patterns related to the various lithologies. Meanwhile, the uranium, thorium and potassium composite images emphasize the radioelement distribution and highlight areas where a particular radioelement has a relatively higher concentration. Choice of the above-mentioned combinations of the radiospectrometric variables takes into consideration the main objectives of the present study. The red, green and blue (RGB) colour combination was used to produce these composite images.

(1) Absolute radioelement composite image:

Different rock types have different characteristic concentrations of the three main radioelements. Therefore, concentrations calculated from gamma-ray spectrometric data can be used to identify zones of consistent lithology and contacts between constraining lithologies. The absolute three radioelement composite image map (fig. 14) of the study area shows variations occurring in the composite three radioelement concentrations, which mainly reflect lithologic variations. This map is a three-element display of eU (in red), eTh (in green) and K (in blue). The colour index at each corner of the triangular legend indicates 100% concentration of the indicated radioelement. The colour at each point inside the triangle represents different ratios of the radioelements according to their colour differences on the absolute three radioelement composite image map.

The image given in Fig. (14) offers much in terms of lithologic variations and shows a fairly close spatial correlation with the geologically mapped lithologies in many locations of the study area. This correlation indicates that the resulting radioelement concentrations are usually representative of the underlying lithology. The granitic rocks of Umm-Zarabit pluton, Dokhan volcanics and Hammamat sediments are clearly visible on the absolute radioelement composite image map (Fig. 14) and can be easily discriminated from the adjacent rocks. Meanwhile, this map does not give much help towards providing colour discrimination between some of the lithologically mapped units as the Middle Miocene, Post Hammamat felsites, Mesozoic Nubian group, Lower Eocene and Upper Cretaceous. This may be attributed to their relatively small area of exposure as well as the limited variations between their gamma-ray responses.

It was noticed that the red colour, which is indicative of the eU concentration on the radioelement composite image (Fig. 14), is common essentially in three zones; in the northern part of the study area to the northwest of W. Umm Esh, in the southern part to the west of W. Umm Zarabit and in the northwestern corner to the north of W. Abu-Aqarib. These zones are clearly correlated mainly with the Upper Cretaceous, Middle Miocene and Younger granites. The areas with higher concentration of the three radioelements (bright areas on Fig. 15) are associated with the granitic rocks occupying the eastern and north western parts of the mapped area, as well as with the wadi sediments in the southwestern part. Low eU, eTh and K concentrations (black areas on Fig. 14) could easily be distinguished mainly in the central and northwestern corner of the mapped area associated with the Dokhan volcanics, Middle Miocene and wadi sediments.

(2) eU composite image:

The relative concentration of uranium with respect to both potassium and thorium is an important diagnostic factor in the recognition of probable uranium deposits (IAEA, 1988). The uranium composite image map (Fig. 15) provided useful information regarding the identification of preferential zones of enriched uranium concentration, which could provide good prospects for further uranium exploration. These images also reflect lithological differences and could be useful in geological mapping problems (Dickson and Scoot, 1997). The eU composite image map is made up of eU concentration (in red) with the two ratios eU/eTh (in green) and eU/K (in blue). These radioelements when combined together generate white areas representing zones with high uranium concentrations. Close inspection of this image (Fig. 15) shows that such areas are well correlated with the Upper Cretaceous, Middle Miocene and younger granitic rocks located principally in three main sites occupying the northern, northwestern and south central parts of the study area. Most of these uranium enrichment zones are associated with the phosphatic beds of the Upper Cretaceous sediments. These phosphate related uranium anomalies are not only attractive in terms of their uranium content, but also due to the fact that they would make the development of the phosphates and uranium together more economically feasible. Meanwhile, the dark areas (with low relative uranium values) on this map (Fig. 15) are associated mainly with the Dokhan volcanics and Hammamat sediments. These zones are limited in their spatial distribution forming local scattered spots, which may reflect inhomogenities in the composition of the corresponding lithological units.

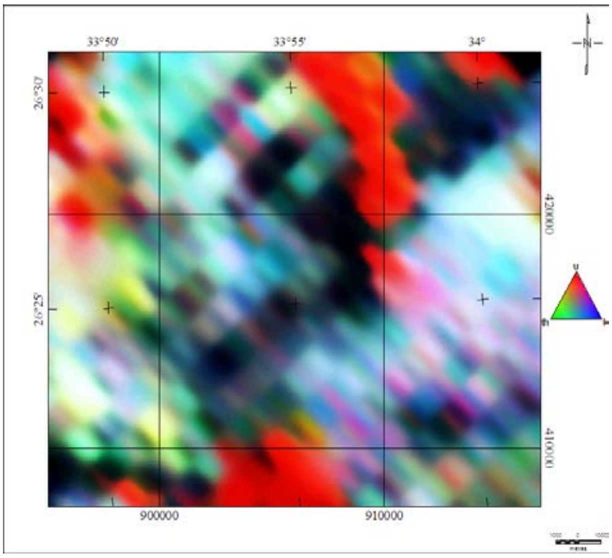

Fig. (14): False colour radioelement composite imagemap, G. Umm Zarabit area, Central Eastern Desert, Egypt.

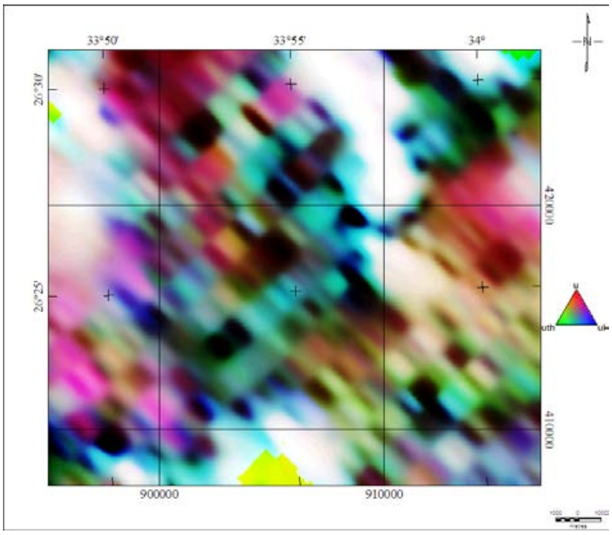

Fig. (15): False colour eU composite image map, G. Umm Zarabit area, Central Eastern Desert, Egypt.

(3) eTh composite image:

The thorium composite image map (Fig. 16) emphasizes the relative distribution of eTh and highlights areas of thorium enrichment. This map combines eTh (in red), eTh/eU (in blue) and eTh/K (in green). Bright colour on this image is a good pointer to areas where thorium has been preferentially enriched relative to potassium and uranium. Such areas could be representing a good prospect for deposits of heavy mineral placers and rare earth elements (Duval, 1983). These bright-coloured zones are associated mainly with the younger granitic rocks located essentially in the northwestern part of the mapped area to the north of W. Abu Shiqeili and in the northeastern part north of W. Abu Safi. Moreover, such enriched thorium concentration zones are encountered also in the western part of the area to the north of W. Abu Saqia, associated with wadi alluvium. Similar to the eU composite image map, it was noticed that the dark areas (representing the low relative thorium values) are also related to the Dokhan volcanics and Hammamat sediments occupied mainly the central and northwestern parts of the study area.

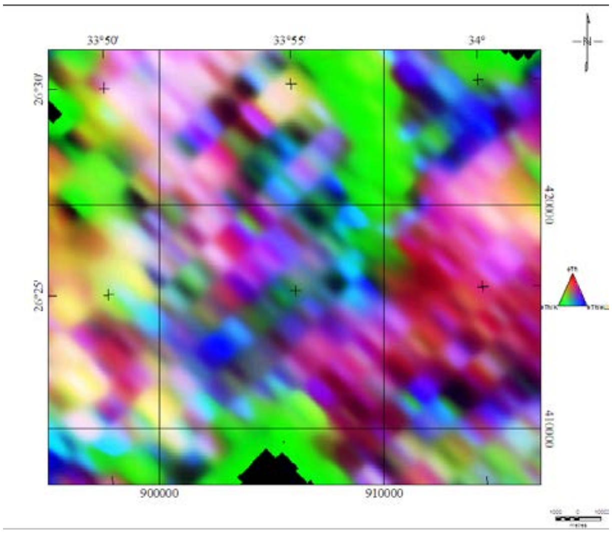

Fig. (16): False colour eTh composite image map, G. Umm Zarabit area, Central Eastern Desert, Egypt.

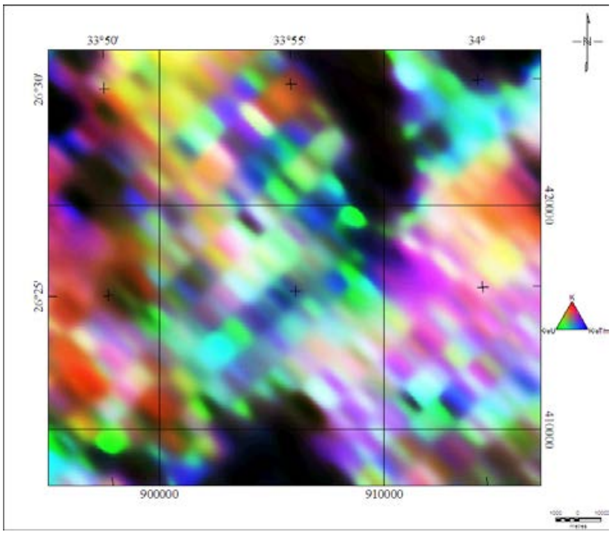

Fig. (17): False colour K composite image map, G. Umm Zarabit area, Central Eastern Desert, Egypt.

(4) K composite image:

The potassium image map (Fig. 17) shows the overall spatial distribution of the relative potassium concentrations and highlights areas with higher potassium contents compared to both uranium and thorium. It also indicates areas where hydrothermal alterations associated with potassium enrichment might have occurred (Duval, 1983). This map combines K (in red) with the two ratios K/eU (in green) and K/eTh (in blue). High relative potassium concentration can be distinguished on the potassium composite image map as anomalous bright zones (high values). These anomalous zones are spatially correlated with the Dokhan volcanics and younger granitic rocks, which occur as small scattered areas occupying the central and eastern parts of the area. The dark zones on this image (low relative potassium values) are associated with the Upper Cretaceous and Middle Miocene sediments located in the northern, south central and northwestern parts of the study area.

CONCLUSIONS

The present study deals with the integration between the aeroradiospectrometric and the geologic data essentially to identify the significant zones of anomalously high radioelement concentrations. The study shows that there is a close relationship between the distribution of the radioelements and the lithology. The interpretation of the gamma-ray spectrometric survey data of the study area proved that their radiation levels, in general, are relatively low since they recorded 23.54 Ur, 3.49%, 15.25 ppm and 18.78 ppm as maximum values for T.C., K, eU and eTh, respectively. However, for many reasons, the interpreted anomalous zones can't be counted as of no significance and are to be ignored, but follow-up investigations are warranted over all of these sits.

Generation and interpretation of the false-colour composite image outlined probable potential zones of high radioelement content, which could be suitable targets for radioactive mineral exploration. These zones are located essentially in three zones; in the northern part of the study area to the northwest of W. Umm Esh, in the southern part to the west of W. Umm Zarabit and in the northwestern corner to the north of W. Abu-Aqarib. These zones are clearly correlated mainly with the Upper Cretaceous, Middle Miocene and Younger granites.

Calculation of the U, Th and K-favourability indices has been carried out for the various rock units to locate rocks having the highest radioelement potentialities. The values of these indices were found to oscillate from 0.74 to 5.21, from 0.78 to 1.20 and from 9.47 to 22.37 for U, Th and K respectively. The younger granites together with the Post Hammamat felsites and Hammamat sediments represent the most favourable rock types for uranium potentiality.

The application of uranium migration technique revealed that the maximum amount of uranium migration-out (depletion) rate is connected with the younger granites, Post Hammamat felsites and Hammamat sediments, which indicate that they could be represented as major U-source bodies in the study area. Meanwhile, Upper Cretaceous together with Lower Eocene sediments and Quaternary alluvium could be considered as uranium migration-in (enrichment) units.

REFERENCES

Aero Service (1984): Final operational report of airborne magnetic/radiation survey in the Eastern Desert, Egypt, for the Egyptian General Petroleum Corporation, Cairo, Egypt. Aero Service, Houston, Texas, USA, April, 1984, Six Volumes.

Akkaad, M.K., and Noweir, A.M. (1980): Geology and Lithostratigraphy of the Arabian Desert Orogenic Belt of Egypt between Lat. 25^o 30$'$ and 26^o 30$'$ N. Inst. Applied Geol., Jeddah, King Abdulaziz Univ., Saudi Arabia, Bull.3, V.4, pp.127-135.

Ammar, A.A., El-Sadek, M.A., and Sabri, A.M. (1999): Utilization of aeroradiospectrometric survey data in defining radioelement anomalies zones in Elgalala Elbahariya – Elgalala Elqibliya area, Northern eastern Desert, Egypt. Vol. 2, pp.315-339, the First International Conference on the Geology of Africa, Assiut Univ., Egypt.

Benzing uranium institute (1977): Field gamma-ray spectrometric survey. No.3, 1-292, China.

Broom, H.J. (1990): Generation and interpretation of geophtsical images with examples from the Rae Province, Northwestern Canada Shield. Geophysics, Vol. 55, No. 8, pp. 977-997.

Conoco (1986): Photogeological interpretation map of Gulf of Suez “sheet 14”, Scale 1:100, 000., Egypt. Prepared by Conoco Inc. in collaboration with Free University, Berlin.

Conoco Coral (1989): Stratigraphic Lexicon and explanatory notes on the geological map of Egypt, Scale 1:500,000. By: M. Hermina, E. Klitzsch and K.L. Franz, Egypt. 236p.

Darnley, A.G., Charbonneau, B.W., and Richardson, K.A. (1977): Distribution of uranium in rocks as a guide to the recognition of uraniferous regions. In Recognition and Evaluation of Uraniferous Areas, Proc. Series, IAEA, Vienna, Austria, p.55-86.

Dickson. B.L. and Scoot, K.M. (1997): interpretation of aerial gamma-ray surveys-adding the geochemical factors. AGSO Journal of Australian Geology and Geophysics, 17 (2), pp.187-200.

Duval, J.S. (1983): Composite colour images of aerial gamma-ray spectrometric data. Geophysics, V., pp. 722-735.

Egyptian Geological Survey and Mining Authority "EGSMA" (1978): Geological maps of the Qena Quadrangle, Scale 1:500,000. Geol. Surv. of Egypt. Cairo, Egypt.

El-Gaby, S., List, F.K., and Tehrani, R. (1988): Geology, evaluation and metallogenesis of the Pan-African belt in Egypt, in the Pan-African belt of Northeast Africa and adjacent areas. Ed. by S. El-Gaby and R.O. Greiling, pp.17-68, Friedr. Vieweg, Braunschweig, Federal Republic of Germany.

El-Gaby, S., List, F.K., and Tehreni, R. (1990): The basement complex of the Eastern Desert and Sinai, Egypt. In the Geology of Egypt. Ed. By Said, R., Published by Balkema, A.A., Rotterdam, Netherlands, pp.175-181.

El-Shazly, E.M. (1977): The geology of the Egyptian region. In the Ocean Basins and Margins. Ed. by Nairn, A.E.M., Kanes, W.H., and Stehli, F.G., Plenum Publishing Corporation, pp.379-444.

El-Shazly, E.M., Dixon, T.H., Engel, A.E.J., Abdelmeguid, A.A., and Stern, R.J. (1980): Late Precambrian crustal evolution of Afro-Arabian from Oceanic Arc to Craton. Egypt. Jour. Geol., 24/1-2, pp101-121.

Elsirafy, A.M., Nielsen, A.A., and Conradsen, K. (1994): Application of image processing techniques and geostatistical methods to the aerial gamma-ray spectrometric and magnetometric survey data of a sample area from the Central Eastern Desert of Egypt as an aid to geological mapping and mineral exploration. Institute of Mathematical Modelling, Technical Univ. of Denmark, Image Analysis Group, 94p.

International Atomic Energy Agency (1988): Geochemical Exploration for uranium. Technical Report series, No.284, Vienna, Austria, 97p.

International Atomic Energy Agency (2003): Guidelines for radioelement mapping using gamma-ray spectrometric data. TECDOC-1363, IAEA, Vienna, Austria, 172p.

Nuclear Materials Authority (NMA) Report (1999): A report of work progression during II sub-stage (December, 1989 – February, 1999) on uranium evaluation in Abu-Zeneima area, Sinai, Egypt. Confidential report, NMA, Cairo, Egypt.

Ong, Y.H. and Mior Shallehhuddin, B.M.J. (1988): Promising uranium the Central Belt area, Peninsular Malaysia, in uranium deposits in Asia and the Pacific: Geology and Exploration, Vienna, Austria, pp.97-107, prospects in IAEA-Tc-543/7.

Pitkin, J.A., and Duval, J.S. (1980): Design parameters for aerial gamma-ray surveys. Geophysics, V.45, No.9, pp.1427-1439.

Sarma, D.D., and Koch, G.S. (1980): A statistical analysis of exploration geochemical data for uranium. Mathematical Geology, V.12, No.2. pp.99-114.

Saunders, D.F., and Potts, M.J. (1978): Manual for the application of NURE 1974-1977 aerial gamma-ray spectrometer data; U.S. Dept. of Energy, Grand Junction Office, Report GJBX-13(78).